PROCEEDINGS OF THE ROYAL SOCIETY B

rspb.royalsocietypublishing.org

Research

Cite this article: Schweitzer MH, Zheng W, Cleland TP, Goodwin MB, Boatman E, Theil E, Marcus MA, Fakra SC. 2014 A role for iron and oxygen chemistry in preserving soft tissues, cells and molecules from deep time. *Proc. R. Soc. B* **281**: 20132741.
http://dx.doi.org/10.1098/rspb.2013.2741

Received: 21 October 2013
Accepted: 29 October 2013

Subject Areas:
biochemistry, palaeontology, cellular biology

Keywords:
soft tissue preservation, haemoglobin, iron, goethite, Fenton chemistry, protein cross-linking

Author for correspondence:
Mary H. Schweitzer
e-mail: mhschwei@ncsu.edu

†Present address: The Department of Biomedical Engineering, Rensselaer Polytechnic Institute, Troy, NY 12182, USA.
‡Present address: American Association for the Advancement of Science, Arlington, VA, USA.

Electronic supplementary material is available at http://dx.doi.org/10.1098/rspb.2013.2741 or via http://rspb.royalsocietypublishing.org.

Royal Society Publishing

A role for iron and oxygen chemistry in preserving soft tissues, cells and molecules from deep time

Mary H. Schweitzer[1,2], Wenxia Zheng[1], Timothy P. Cleland[1,†], Mark B. Goodwin[3], Elizabeth Boatman[4,‡], Elizabeth Theil[5,6], Matthew A. Marcus[7] and Sirine C. Fakra[7]

[1]Marine, Earth, and Atmospheric Sciences, North Carolina State University, Campus Box 8208, Raleigh, NC 27695, USA
[2]North Carolina Museum of Natural Sciences, 11 West Jones Street, Raleigh, NC 27601, USA
[3]Museum of Paleontology, and [4]Department of Material Sciences and Engineering, University of California, Berkeley, CA 94720, USA
[5]CHORI (Children's Hospital Oakland Research Institute), 5700 Martin Luther King, Jr. Way, Oakland, CA 94609, USA
[6]Department of Molecular and Structural Biochemistry, North Carolina State University, Raleigh, NC 27695-7622, USA
[7]Advanced Light Source, Lawrence Berkeley National Laboratory, Berkeley, CA 94720, USA

The persistence of original soft tissues in Mesozoic fossil bone is not explained by current chemical degradation models. We identified iron particles (goethite-αFeO(OH)) associated with soft tissues recovered from two Mesozoic dinosaurs, using transmission electron microscopy, electron energy loss spectroscopy, micro-X-ray diffraction and Fe micro-X-ray absorption near-edge structure. Iron chelators increased fossil tissue immunoreactivity to multiple antibodies dramatically, suggesting a role for iron in both preserving and masking proteins in fossil tissues. Haemoglobin (HB) increased tissue stability more than 200-fold, from approximately 3 days to more than two years at room temperature (25°C) in an ostrich blood vessel model developed to test post-mortem 'tissue fixation' by cross-linking or peroxidation. HB-induced solution hypoxia coupled with iron chelation enhances preservation as follows: $HB + O_2 > HB - O_2 > -O_2 \gg +O_2$. The well-known O_2/haeme interactions in the chemistry of life, such as respiration and bioenergetics, are complemented by O_2/haeme interactions in the preservation of fossil soft tissues.

1. Introduction

Preservation of structures in fossils that were not *originally* mineralized in the living organisms is uncommon, but is represented in microbes, plants and animals in disparate environments throughout the fossil record (e.g. [1] and references therein). Soft tissue structures retaining some aspects of original material, and thus not completely replaced replicas, have been described in Mesozoic fossil bone as early as the 1960s [2–5]. This 'exceptional preservation' has been observed for decades, but is not addressed by models of fossilization processes wherein an organism is buried and degraded, and spaces left by degrading organics are subsequently filled by precipitation of exogenous minerals. Modes of preservation to explain the persistence of these secondarily mineralized, but originally soft tissues include microbially mediated stabilization [6,7], early diagenetic mineralization or authigenic replacement [8–10], 'sulfurization' [11,12] and others (reviewed in [6,13,14]), but few of these preservation modes have been experimentally tested.

Recently, still-soft biomaterials have been identified in bones of multiple taxa from the Cretaceous to the Recent, with morphological and molecular characteristics consistent with an endogenous source [15–20]. An alternative hypothesis, that these structures result from microbial biofilms [21], is *eliminated* by several

lines of evidence, including but not limited to: (i) immunological reactivity (multiple antibodies binding both with chemical extracts and *in situ*, independent of contributions from, and not reactive to, biofilms [17,22,23]); (ii) peptide sequence data from proteins not found in microbes [17,22–25]; and (iii) identification of histones—nuclear, chromosomal proteins that are eukaryote-specific—by both amino acid sequence and antibody localization [22]. Multiple lines of evidence support the endogeneity of these recovered molecules in Cretaceous specimens, despite hypothesized temporal limits on molecular preservation of less than 1 Myr for proteins and approximately 100 000 years for DNA [26–30] (but see [31]) that are based upon degradation proxies of heat and/or pH [28,32], theoretical models of breakdown kinetics [33,34], and, recently, extrapolation from a select and time-limited set of fossils [35]. For soft tissues and the proteins comprising them to persist beyond these limits, a mode of preservation sufficiently rapid to outpace decay is required [6]. Here, we propose a chemical explanation for molecular and tissue 'fixation' over time involving iron-catalysed free-radical reactions.

Redox-active iron, abundant in living cells and tissues, is stabilized in haeme proteins (e.g. haemoglobin (HB), myoglobin, cytochromes [36–39]), non-haeme iron proteins (e.g. ribonucleotide reductase, fatty acid desaturase [40]) and ferritin, a protein which synthesizes iron oxyhydroxide mineral nanoparticles [41,42]. These proteins control the rapid generation of oxygen-free radicals by environmental dioxygen (O_2) [42–44]. Although approximately 85% of iron in animals resides in HB [45], thousands of iron atoms are also sequestered in life in a single ferritin molecule [46]. When iron–protein binding is disrupted through death or disease [47–49], iron-induced Fenton-type reactions occur, producing insoluble (K_s approx. 10^{-18} M) mineralized iron/rust and highly reactive hydroxyl radicals [37,42,50,51]. Ferritin is a complex protein that synthesizes iron biominerals, the form of which is environmentally dependent. In its antioxidant mode, ferritin scavenges cytoplasmic iron (II) and sequesters it as protein-caged, iron biomineral [41]. Nevertheless, some iron escapes, contributing to formation of oxy radicals that amplify peroxidation of membrane lipids [43,50,52,53]. Oxy radicals also facilitate protein cross-linking [54] in a manner analogous to the actions of tissue fixatives (e.g. formaldehyde), thus increasing resistance of these 'fixed' biomolecules to enzymatic or microbial digestion [55,56]. Lipid peroxidation and protein condensation reactions are harmful to living tissues [52,54], but could act to preserve tissues and biomolecules after death.

Here, we show data from both fossil and extant organic material to support the hypothesis that iron contributes to preservation of soft tissues and molecules. We present direct evidence that iron is closely associated with still-soft tissues (e.g. semi-transparent, pliable 'vessels', osteocyte-like microstructures and associated contents) recovered from fossils using our aseptic protocols [17,22]; and that treatment of these materials with the iron chelators pyridoxal isonicotinic hydrazide (PIH [57]), salicylaldehyde isonicotinic hydrazide (SIH [58,59]) or polyethylene glycol 600 (PEG600 [60]) increased antibody recognition *in situ*, with PIH the most efficient and least damaging to tissues.

When extant, post-mortem ostrich blood vessels were incubated in a red blood cell lysate rich in solubilized HB, iron deposits formed quickly and these materials have resisted tissue degradation for many months at room temperature with no further treatment (see the electronic supplementary material). We also compared vessels in aerobic or hypoxic conditions and found that tissues incubated in HB in the presence of dioxygen displayed the greatest stability and longevity, to date more than 2 years.

2. Material and methods

For details of actualistic experiments and additional figures (S1–S6), see the electronic supplementary material.

3. Results

Transmission electron microscopy (TEM) shows iron intimately associated with vessels recovered from demineralized dinosaur tissues (figure 1). Both isolated *Tyrannosaurus rex* (MOR 1125) vessels (figure 1*a*,*c*,*e*) and *Brachylophosaurus canadensis* (MOR 2598) vessels (figure 1*b*,*d*) show iron-rich nanoparticles, often embedded in an amorphous, apparently 'organic' layer that is sometimes almost completely obscured by electron-dense iron particles (figure 1*b*). Figure 1*c* shows a structure protruding into the lumen of the dinosaur vessel that is similar in morphology to nuclei of the endothelial cells (EN) that comprise extant ostrich vessel walls (figure 1*f*). Higher magnification of the boxed region in figure 1*c* shows the intimate relationship between the organic layer and iron (figure 1*e*). Lower magnification of an ostrich vessel in cross section (figure 1*f*) shows distinct EN-containing chromatin protruding into the lumen of the vessel and a tight junction (TJ) uniting two cell membranes. The tapering nature of the endothelial cell (EC) cytoplasm is clearly visible, and is consistent with structures seen under higher magnification of *T. rex* vessels (figure 1*c*).

Figure S1 in the electronic supplementary material shows backscatter TEM images of isolated osteocytes [22] of *T. rex* (electronic supplementary material, figure S1*A*) and *B. canadensis* (electronic supplementary material, figure S1*C*). Electron energy loss spectroscopy (EELS) elemental maps show iron localized to cells and intracellular contents of both dinosaurs (electronic supplementary material, figure S1*B*,*D*). When these cells were treated to chelate iron, EELS shows that iron signal is greatly decreased and more diffuse (electronic supplementary material, figure S2). This supports the intimate association of iron to these preserved, still-soft structures.

Synchrotron microprobe techniques were used to investigate dinosaur and ostrich vessels, intravascular material and chemical speciation of associated iron. Micro-X-ray fluorescence (μ-XRF) distribution maps of iron at 3 μm resolution (red pixel intensity corresponds to iron concentration) are shown in extended regions of HB-incubated ostrich (figure 2*a*), *B. canadensis* (figure 2*b*) and *T. rex* (figure 2*c*) vessel samples, which had been air-dried on an Si_3N_4 window (Silson). In all cases, iron was found in intimate association with the vessel structures. Micro-X-ray absorption near-edge structure (μ-XANES) spectroscopy was used to determine the chemical speciation of iron at multiple locations on each sample (white numerical labels), with representative plots of the corresponding spectra shown in figure 2*d–f* for HB-incubated ostrich, *B. canadensis* and *T. rex*, respectively. In each Fe μ-XANES plot, the experimental spectrum is in black, the corresponding least-square linear combination fit is displayed in red, and green shows the residuals. The chemical speciation of iron in the HB-incubated ostrich tissue was a combination of oxyhaemoglobin and a disordered Fe oxyhydroxide, which was

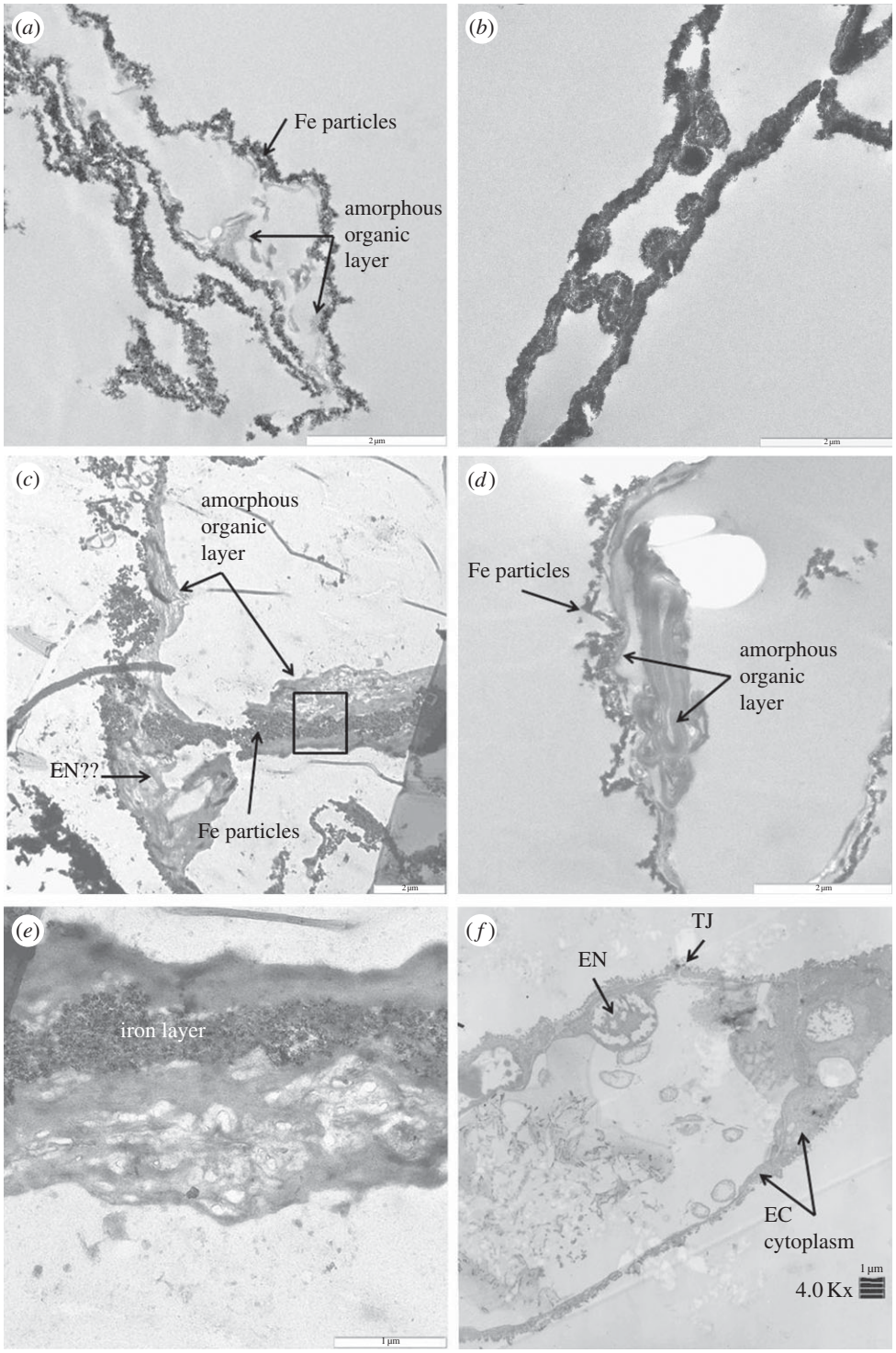

Figure 1. TEM images of (*a*,*c*,*e*) *T. rex* (MOR 1125) vessels, (*b*,*d*) *B. canadensis* (MOR 2598) vessels and (*f*) ostrich vessels. *Tyrannosaurus rex* vessels show iron particles infiltrating a relatively amorphous 'organic' layer (arrows, *a*,*c*). Higher magnification (*c*) shows a structure similar in morphology to an endothelial cell nucleus seen in ostrich vessel (EN, *f*), protruding into the lumen of an isolated vessel. No chromatin or nuclear membrane is visible in the dinosaur structures, but these features are visible in the ostrich. (*e*) Higher magnification of the area within the box in (*c*) shows variation in texture within the 'organic' layer. *B. candensis* vessels are more completely infiltrated with iron (*b*), but in some views (*d*), an organic layer is still visible. The ostrich vessel (*f*) shows nuclear membrane (EN) within the endothelial cell (EC). Cytoplasmic extensions make up the bulk of the vessel wall, and a TJ uniting two endothelial cells. Scale bar, 2 µm for (*a*–*d*), 1 µm for (*e*,*f*).

represented in fits by biogenic Fe oxide [61] and which will be referred to hereafter as 'biogenic-like oxide' (BLO). Both dinosaur tissues were found to contain a combination of goethite (α-FeO(OH)) and biogenic iron oxyhydroxide.

Optical microscopy was used to identify intravascular material in the vessels of *B. canadensis* (figure 2*g*) and *T. rex* (figure 2*k*). µ-XRF mapping revealed high concentrations of iron in these intravascular structures (figure 2*h*,*l*, respectively). Micro-X-ray diffraction (µ-XRD) analysis of intravascular structures in the dinosaur vessels identified these features as crystalline goethite (figure 2*i* at location 1 and figure 2*m* at location 13). Iron µ-XANES performed at the same locations showed that, in addition to crystalline goethite, these locations also contained highly disordered amorphous (i.e. poorly diffracting) iron oxyhydroxides best matching a biogenic iron oxyhydroxide standard. Similar accumulations

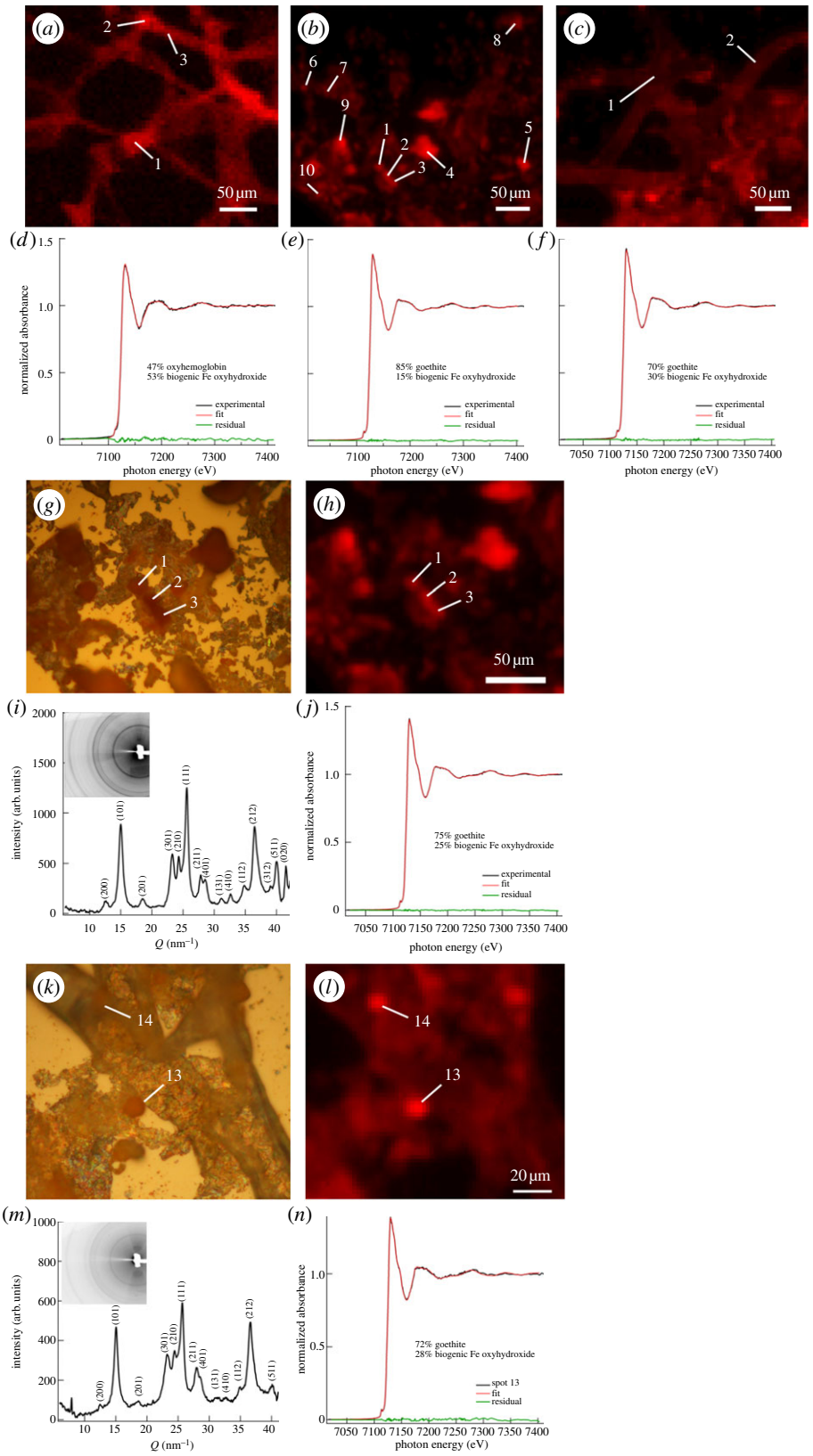

Figure 2. (*a–c*) µ-XRF maps of HB-incubated ostrich, *B. canadensis* (MOR 2598) and *T. rex* (MOR 1125) vessel tissues at 3 µm resolution, with locations of analysis identified by white numerical labels, illustrating the intimate association of Fe with each vessel tissue. (*d–f*) µ-XANES analysis of iron chemical speciation at representative locations, respectively, for each vessel tissue, where the experimental data are plotted in black and the least-square linear combination fits are in red. HB-incubated ostrich tissue was found to contain iron in the form of oxy-HB and biogenic (disordered non-crystalline) iron oxyhydroxide; by contrast, dinosaur vessels contained goethite (α-FeO(OH)) in addition to disordered biogenic-like oxide (BLO) iron oxyhydroxide. Green curves are residuals and indicate good fits for all three samples. (*g,h*) Optical microscopy, µ-XRF analysis of intravascular structures in *B. canadensis*. (*i,j*) µ-XRD and iron µ-XANES chemical analysis of intravascular structure (location 1) in *B. canadensis* identifies these features as crystalline goethite with an additional fraction of biogenic iron oxyhydroxide, which is amorphous (i.e. poorly diffracting). (*k–n*) Investigation of intravascular structures in *T. rex* revealed similar findings (i.e. location 13 was identified as a combination of goethite and biogenic Fe oxyhydroxide). Whole pattern µ-XRD insets of (*i,m*) exhibit thin, continuous rings for both *B. canadensis* and *T. rex*, indicating that the goethite in both samples is nanocrystalline. Labels associated with peaks (e.g. 200, 101) represent *h*, *k*, *l* Miller indices of diffracting planes. XRD was used to identify the nature of the crystalline iron oxyhydroxides and XANES spectroscopy was used to probe the poorly crystalline or amorphous (i.e. poorly diffracting) phase(s) using least-square linear combination fitting and a set of iron standards. (Online version in colour.)

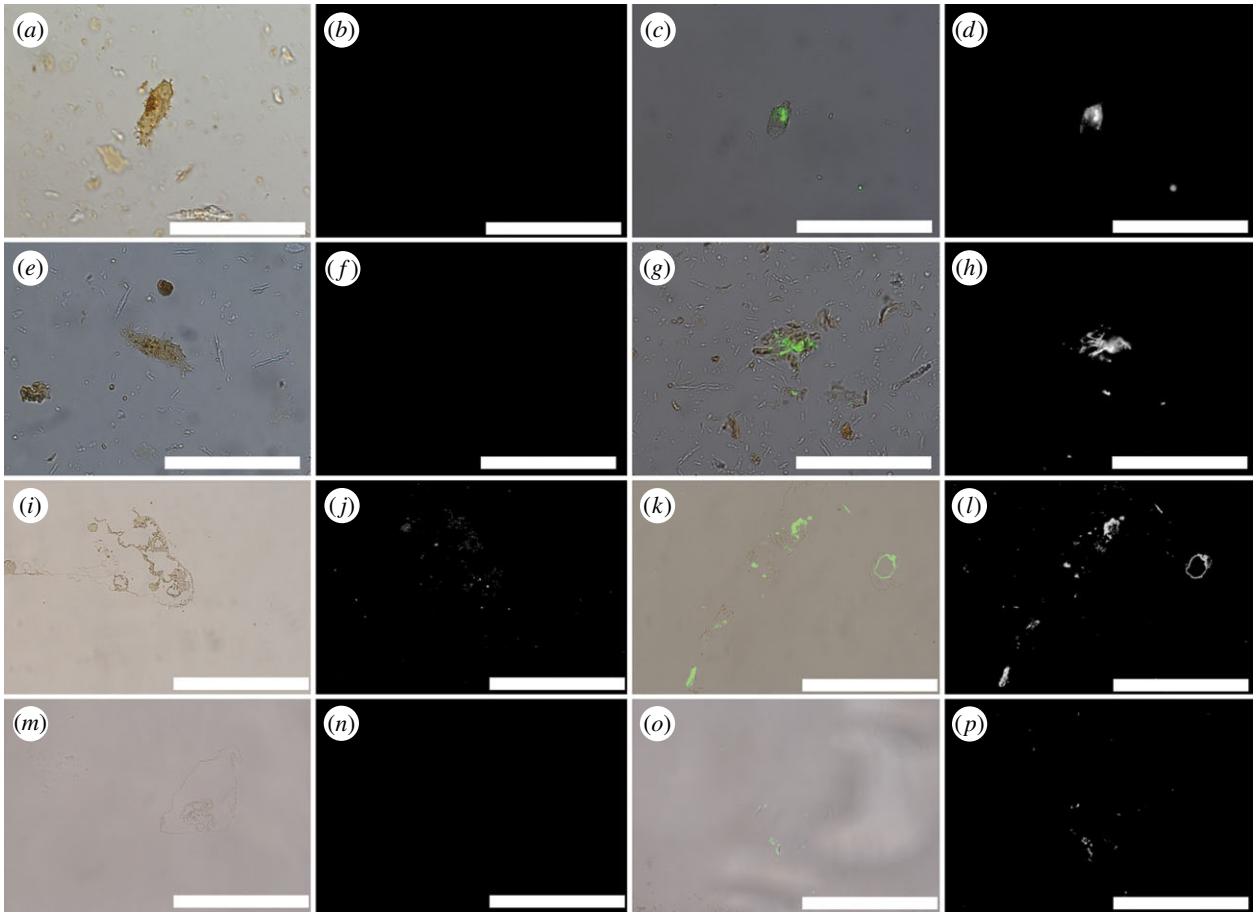

Figure 3. Overlay and fluorescence microscopy images of dinosaur 'osteocytes' and vessels after exposure to polyclonal antibodies. (*a–h*) Cells exposed to antibodies against actin protein; (*i–p*) vessels exposed to antibodies raised against elastin protein, a component of vessel walls. (*a*,*b*) *Brachylophosaurus canadensis* and (*e*,*f*) *T. rex* osteocytes show minimal reactivity to antibodies before treatment with PIH; treatment with the iron chelator PIH result in increase in binding to actin antibodies in both *B. canadensis* (*c*,*d*) and *T. rex* (*g*,*h*) isolated osteocytes. Similar increase in antibody binding is visible in dinosaur vessels. (*i*,*j*) isolated vessel from *B. canadensis* exposed to elastin antibodies without PIH; binding is greatly increased after chelation (*k*,*l*). A similar pattern is seen for *T. rex* vessels before (*m*,*n*) and after chelation (*o*,*p*). All data collection parameters are identical for each condition. Scale bar is 50 µm for each image. (Online version in colour.)

of iron were observed in HB-treated ostrich vessels, as shown in figure 2*a*, locations 1 and 2, which is in contrast to the amorphous pattern of the ostrich vessel tissue observed at regions of low iron concentration (e.g. location 3 in figure 2*a*; electronic supplementary material, figure S3). However, all analysed regions of *B. canadensis* and *T. rex* vessels exhibited finely crystalline character (thin, continuous rings in whole pattern insets of figure 2*i*,*m*), suggesting that these vessel tissues are associated with nanocrystalline goethite.

Iron chelation increased immunoreactivity of proteins in osteocytes and vessels of dinosaurs [17,22,23]. Dinosaur osteocytes had minimal response to anti-actin antibodies before chelation (figure 3*a*,*b*,*e*,*f*), but responses increased dramatically after iron chelation (figure 3*c*,*d*,*g*,*h*). When vessels from both dinosaurs were exposed to elastin antibodies, a highly conserved protein found in vessel walls of all extant vertebrates [62] (figure 3*i–p*), chelators also enhanced binding over untreated tissues. Both SIH and PIH resulted in increased signal in vessels recovered from *B. canadensis* (figure 3*i–l*) and *T. rex* (figure 3*m–p*), but PIH was most effective, and only data from this chelation treatment are presented.

An ostrich blood vessel model was used to determine post-mortem conditions, possibly contributing to preservation of tissues, as observed in the dinosaur samples. Ostrich vessels were incubated in a concentrated solution of red blood cell lysate (see the electronic supplementary material) to approximate post-mortem erythrocyte lysis. Control tissues were prepared identically, then incubated in either sterile distilled water or phosphate buffered saline (PBS). Haemoglobin was chosen to test its preservation properties for four reasons: (i) HB is in known to be bacteriostatic [63,64]; (ii) in the presence of dioxygen, HB produces free radicals [65]; (iii) blood vessels fill with large amounts of HB after death as red cells begin to die and lyse, thus it is naturally present in large vertebrates [45]; and (iv) haeme released from HB, when degraded, will release iron, possibly accounting for the iron particles associated with preserved soft tissues [42,66] (figure 1).

HB-treated vessels have remained intact for more than 2 years at room temperature with virtually no change, while control tissues were significantly degraded within 3 days. Indicators of tissue stability include thick vessel walls (figure 4*a*,*b*, black arrows) and visible surface structures consistent with endothelial nuclei (figure 4*a*,*b*, white arrowheads). In many cases, material could be seen inside the vessel lumen, appearing most often as structureless masses (figure 4*a*,*b*, asterisk). There was no difference between tissues incubated in HB/hypoxy and HB/oxy conditions (see the electronic supplementary material), including the presence of the intravascular material, except that distinct red blood cells were also present in the HB/oxy condition (figure 4*c*,*d*, asterisk). By contrast, the absence of HB resulted in extensive tissue degradation, indicated by bacilliform bacteria (figure 4*h*, asterisk), fungal

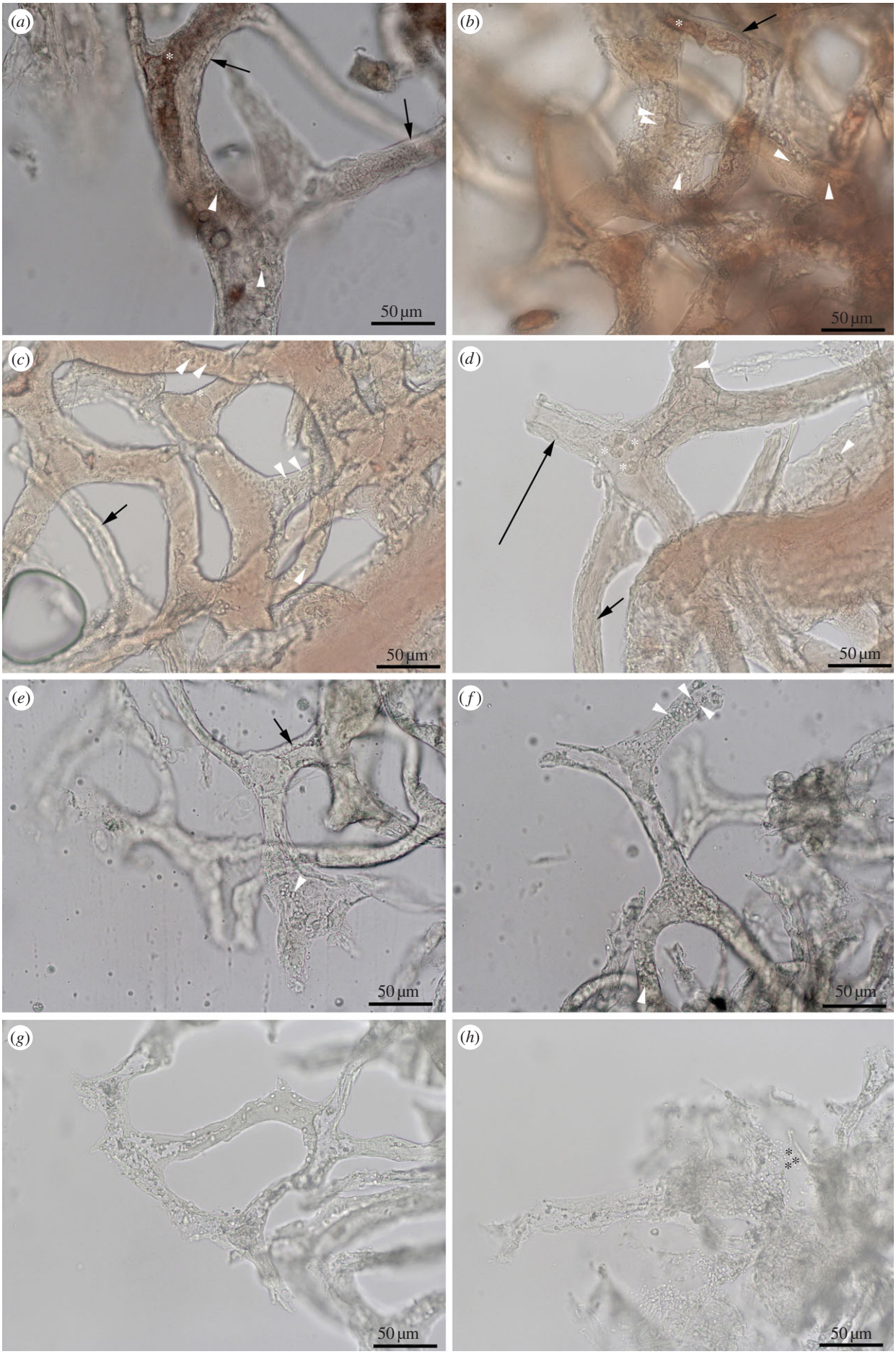

Figure 4. Ostrich vessels isolated from extant bone. (*a*,*b*) Vessels incubated in HB in deoxygenated condition; (*c*,*d*) vessels incubated in HB, but exposed to oxygen. (*e*,*f*) Deoxygenated vessels incubated in distilled water; (*g*,*h*) vessels incubated in distilled water and oxygenated. Black arrows show endothelial layer is much thicker and better preserved in HB-soaked vessels. Other details are seen in HB vessels, for example possible endothelial nuclei on vessel surfaces (white arrowhead). White asterisks indicate red blood cells within vessel of only HB-oxygenated condition; black asterisks show microbial invasion. Scale bar as indicated. (Online version in colour.)

invasion, vessel wall thinning and collapse (figure 4*e*), loss of vessel contents, and complete loss of tissue integrity. Incubation in water or PBS without HB resulted in rapid degradation (approx. 3 days), but when dioxygen was removed with an argon purge, tissue degradation was somewhat delayed. More importantly, ostrich vessels incubated with HB in the presence of oxygen were bright red (light microscopy) (figure 4*c*,*d*), while those in the argon-purged (hypoxic) solution were darker (figure 4*a*,*b*), indicating that a haeme–oxygen complex formed and coincided with enhanced tissue stability. The range of tissue stabilities observed with differing combinations of HB and O_2 were: HB + O_2 > HB – O_2 = PBS – O_2 >> PBS + O_2, emphasizing the importance of both HB and oxygen to tissue stabilization.

Ostrich blood vessel structure was stabilized when HB was present, but in the presence of oxygen, degradation was further inhibited relative to the hypoxic state. Scanning electron microscopy (SEM) shows that HB-incubated vessels in the absence of oxygen contain minimal areas of collapse (electronic supplementary material, figure S4*A*,*B*, black arrows) and degradation (electronic supplementary material, figure S3*C*, white arrows) in otherwise intact vessel walls, and endothelial nuclei (white arrowheads) were still visible (electronic supplementary material, figure S4*C*). When both HB and oxygen were present, the blood vessels were fully inflated and there were no areas of collapse, suggesting intact elastin proteins (electronic supplementary material, figure S4*D*). At higher magnification (electronic supplementary material, figure S4*E*,*F*), no regions of breakdown were detected, and surface texture was intact (electronic supplementary material, figure S4*F*).

However, in vessels incubated in PBS/water, tissue degradation was much greater; vessel collapse was less frequently observed in the absence of oxygen (black arrows, electronic supplementary material, figure S4*G*,*I*) than in its presence (electronic supplementary material, figure S4*J*–*L*). This was further evidenced at the end of one month, where microbial contamination was still not observed in either HB condition (electronic supplementary material, figure S5*A*,*B*), but almost completely consumed vessels in both control conditions (electronic supplementary material, figure S5*C*,*D*) after days to weeks. No microbial influence is detected in either HB condition even after storage at room temperature for six months to 2 years.

When ostrich blood vessels were soaked in HB, rinsed and exposed to antibodies against a synthetic HB peptide (NH2-TSLWGKVNVADCGAEALAR-OH) [67] in *in situ* antibody assays, with or without iron chelation, patterns similar to the dinosaur vessels were observed. The ostrich vessels treated with PIH to remove HB-derived iron (electronic supplementary material, figure S6*B*,*D*) showed significantly more antibody binding than those vessels incubated in HB without PIH chelator (electronic supplementary material, figure S6*A*,*C*).

4. Discussion

The HB–oxygen interactions investigated here explain both the association of iron with many exceptionally preserved fossils and the enhanced preservation of tissues, cells and molecules over deep time. Iron and oxygen chemistry, at the centre of bioenergetics and terrestrial life [41], are now seen to play key roles in the preservation of biomaterials after death.

The hypothesis that iron contributes to preservation in deep time, perhaps by both free-radical-mediated fixation and anti-microbial activity, is supported by data presented herein. Although the exact mechanism of microbial inhibition by HB is not known, it has been noted in earlier works [63,64]. The iron may be directly protecting proteins by blocking active sites recognized by enzymes of degradation (supported by the increase in antibody signal after treatment with iron chelator), or it may be providing protection indirectly by binding to oxygen, and thus preventing oxidative damage [68,69] or outcompeting bacterial mechanisms, similar to ferritins [45].

Here, we observe the intimate association between iron (goethite) particles and soft tissues recovered from dinosaurs. In life, blood cells rich in iron-containing HB flow through vessels, and have access to bone osteocytes through the lacuna-canalicular network [70,71]; after death, HB could cause localized, haeme-based radical cross-linking in dinosaur tissues. Moreover, HB-derived haeme, previously identified in dinosaur bone [72], has recently been identified in Miocene mosquitoes, supporting the durability of this prosthetic unit [73]. But are these reactions sufficient to result in long-term preservation?

In our test model, incubation in HB increased ostrich vessel stability more than 240-fold, or more than 24 000% over control conditions. The greatest effect was in the presence of dioxygen, but significant stabilization by HB also occurred when oxygen was absent (figure 4; electronic supplementary material, figure S5). Without HB treatment, blood vessels were more stable in the absence of oxygen, whereas the most rapid degradation occurred with oxygen present and HB absent. Two possible explanations for the HB/O_2 effect on stabilizing blood vessel tissues are based on earlier observations in different environments: (i) enhanced tissue fixation by free radicals, initiated by haeme–oxygen interactions [65]; or (ii) inhibition of microbial growth by free radicals [63,64]. Ironically, haeme, a molecule thought to have contributed to the formation of life [41,74], may contribute to preservation after death.

Goethite-like iron particles similar to those observed in these fossil soft tissues have been identified in modern tissues and are possibly derived from HB through formation of ferritin protein-caged iron biominerals [44,75–79] during degradation. Ferritins are stable proteins that retain activity post-mortem. They are capable of scavenging iron released from less stable proteins and converting it to biominerals such as goethite, depositing it as crystals of relatively uniform size, in surrounding tissues. These iron nanoparticles may have stabilized cell architecture and may even be responsible for preserving intracellular components chemically consistent with DNA [22] through iron-mediated DNA–protein cross-links [80].

However, just as iron contributes to reduction of antibody reactivity (figure 3; electronic supplementary material, figure S5), it may also confound efforts to sequence biomolecules, by diminishing signals in mass spectrometry via ion suppression or by inhibiting enzymes required for DNA sequencing [81,82]. Iron chelation in soft tissue analysis is a technical advance in analysing biomaterials from fossil bone because chelation reduces signal inhibition in many fossil analyses, thus broadening the range of specimens from which molecular data may be obtained.

Biomolecules recovered from fossils have great potential to reveal aspects of the biology and environments of extinct organisms by: (i) independently testing and/or resolving evolutionary relationships determined by morphological

characters; (ii) combining morphological and molecular data from both fossil and extant taxa to generate more robust phylogenies; (iii) illuminating acquisition of physiological strategies not discernible from morphology alone (e.g. cold-adapted HB in *Mammuthus primigenius* [83]); and (iv) providing, independently, estimates on rate and direction of molecular evolution. In addition, molecules derived from fossils can elucidate molecular mechanisms for organismal survival during prolonged periods of global climate change. Finally, studying molecular diversity of organisms in the fossil record before major 'bottleneck' events illuminates population structures and may suggest mechanisms to mitigate the current decline in diversity in some extant lineages.

However, despite this potential, fossils older than approximately 1 Ma have not been targeted for molecular studies, because proposed limits on preservation of organic components in bone [28,30,33,34] obscured the possibility of molecular survival. These models/proxies predict degradation of *tissues* on even shorter time scales. Therefore, the apparent recovery of structures in Cretaceous bone consistent with an endogenous origin that share identical location, texture, morphology, translucency, molecular characteristics and immunoreactivity with extant osteocytes and blood vessels [17,22,24,84] has remained controversial. Here, our data support a naturally occurring mechanism that results in stabilization of these presumably transient components over geological time. Because we observed iron particles in association with soft tissues in these fossils (figure 1), and earlier studies localized iron to the vessels of bone, not the bone matrix or surrounding sediments [72,85,86], we focused our attention on identifying a protein source for iron after death.

Redox reactions of iron are modulated by insertion of iron into porphyrins bound to specific proteins (HB, myoglobin and cytochromes), by integration in iron–sulfur clusters [47,48], or used to synthesize and sequester iron biominerals by ferritins. Multiple cellular repair mechanisms exist to compensate for free-radical-induced damage caused by errant iron (or dioxygen) [55]. After death, iron released from these proteins becomes available for free-radical chemistry with oxygen, leading to protein and lipid cross-linking, tissue fixation and resistance to enzymatic/bacterial degradation [55,56], and also forms particles *in situ* in tissues, as our data demonstrate. Thus, damaging reactions in life can be *preserving* reactions after death. Stabilization of cellular and vascular components by HB iron in solution and/or anoxia in the ostrich vessel model suggests that iron observed in extant and dinosaur tissues is derived from HB degradation. However, other metals also contribute to hydroxyl radical formation; iron may be only one of many metals playing a role in exceptional fossil preservation. Whatever the exact mechanism, iron removal by chelation may increase the number of fossil samples amenable to molecular analyses.

(Note: during the course of review of this manuscript, a paper was published in PNAS [73] that directly relates to our conclusion that iron influences preservation of biomolecules across geological time and speaks of the longevity of some iron-containing biomolecules.)

Acknowledgements. We thank J. Horner, R. Harmon (Museum of the Rockies, Montana State University) and the rest of the palaeontology crew for access to specimens; S. Brumfeld and N. Equall (Montana State University) for TEM and SEM data, respectively; J. Fountain for geochemical discussions and input; North Carolina State University and the NC Museum of Natural Sciences for continued support of our efforts; and colleagues who contributed seed ideas through multiple discussions.

Funding statement. This research was financially supported by the National Science Foundation (DGE-0750733 to T.P.C. and EAR 0541744 to M.H.S.) and the David and Lucile Packard Foundation to M.H.S. The operations of the Advanced Light Source at Lawrence Berkeley National Laboratory are supported by the Director, Office of Science, Office of Basic Energy Sciences, US Department of Energy under contract number DE-AC02-05CH11231.

References

1. Schweitzer MH. 2011 Soft tissue preservation in terrestrial mesozoic vertebrates. *Annu. Rev. Earth Planet. Sci.* **39**, 187–216. (doi:10.1146/annurev-earth-040610-133502)
2. Pawlicki R, Korbel A, Kubiak H. 1966 Cells, collagen fibrils and vessels in dinosaur bone. *Nature* **211**, 655–657. (doi:10.1038/211655a0)
3. Pawlicki R. 1995 Histochemical demonstration of DNA in osteocytes from dinosaur bones. *Folia Histochem. Cytobiol.* **33**, 183–186.
4. Pawlicki R. 1984 Metabolic pathways of the fossil dinosaur bone. Part II. Vascular canal in the communication system. *Folia Histochem. Cytochem.* **22**, 33–42.
5. Pawlicki R, Nowogrodzka-Zagorska M. 1998 Blood vessels and red blood cells preserved in dinosaur bones. *Ann. Anat.* **180**, 73–77. (doi:10.1016/S0940-9602(98)80140-4)
6. Briggs DEG. 2003 The role of decay and mineralization in the preservation of soft-bodied fossils. *Annu. Rev. Earth Planet. Sci.* **31**, 275–301. (doi:10.1146/annurev.earth.31.100901.144746)
7. Raff EC *et al*. 2008 Embryo fossilizaiton is a biological process mediated by microbial biofilm. *Proc. Natl Acad. Sci. USA* **105**, 19 360–19 365. (doi:10.1073/pnas.0801034105)
8. Briggs DEG, Kear AJ, Martill DM, Wilby PR. 1993 Phosphatization of soft-tissue in experiments and fossils. *J. Geol. Soc.* **150**, 1035–1038. (doi:10.1144/gsjgs.150.6.1035)
9. Zhu M, Babcock LE, Steiner M. 2005 Fossilization modes in the Chengjiang Lagerstatte (Cambrian of China): testing the roles of organic preservation and diagenetic alteration in exceptional preservation. *Palaeogeogr. Palaeoclimatol. Palaeoecol.* **220**, 31–45. (doi:10.1016/j.palaeo.2003.03.001)
10. Trinajstic K, Marshall C, Long J, Bifield K. 2007 Exceptional preservation of nerve and muscle tissues in Late Devonian placoderm fish and their evolutionary implications. *Biol. Lett.* **3**, 197–200. (doi:10.1098/rsbl.2006.0604)
11. McNamara M, Orr PJ, Kearns SL, Alcalá L, Anadón P, Peñalver-Mollá E. 2010 Organic preservation of fossil musculature with ultracellular detail. *Proc. R. Soc. B* **277**, 423–427. (doi:10.1098/rspb.2009.1378)
12. McNamara ME, Orr PJ, Kearns SL, Alcala L, Anadon P, Penalver-Molla E. 2006 High-fidelity organic preservation of bone marrow in ca 10 Ma amphibians. *Geology* **34**, 641–644. (doi:10.1130/G22526.1)
13. Butterfield NJ. 2003 Exceptional fossil preservation and the Cambrian explosion. *Integr. Comp. Biol.* **43**, 166–177. (doi:10.1093/icb/43.1.166)
14. Butterfield NJ, Balthasar U, Wilson LA. 2007 Fossil diagenesis in the burgess shale. *Palaeontology* **50**, 537–543. (doi:10.1111/j.1475-4983.2007.00656.x)
15. Schweitzer MH, Wittmeyer JL, Horner JR, Toporski JK. 2005 Soft-tissue vessels and cellular preservation in *Tyrannosaurus rex*. *Science* **307**, 1952–1955. (doi:10.1126/science.1108397)
16. Schweitzer MH, Wittmeyer JL, Horner JR. 2007 Soft tissue and cellular preservation in vertebrate skeletal elements from the Cretaceous to the present. *Proc. R. Soc. B* **274**, 183–197. (doi:10.1098/rspb.2006.3705)
17. Schweitzer MH *et al*. 2009 Biomolecular characterization and protein sequences of the

Campanian hadrosaur *B. canadensis*. *Science* **324**, 626–631. (doi:10.1126/science.1165069)

18. Bell LS, Kayser M, Jones C. 2008 The mineralized osteocyte: a living fossil. *Am. J. Phys. Anthropol.* **137**, 449–456. (doi:10.1002/ajpa.20886)
19. Lindgren J *et al*. 2011 Microspectroscopic evidence of Cretaceous bone proteins. *PLoS ONE* **6**, e19445. (doi:10.1371/journal.pone.0019445)
20. Cadena E, Schweitzer MH. 2012 Variation in osteocyte morphology vs bone type in turtle shell and their exceptional preservation from the Jurassic to the present. *Bone* **51**, 614–620. (doi:10.1016/j.bone.2012.05.002)
21. Kaye TG, Gaugler G, Sawlowicz Z. 2008 Dinosaurian soft tissues interpreted as bacterial biofilms. *PLoS ONE* **3**, e2808. (doi:10.1371/journal.pone.0002808)
22. Schweitzer MH, Zheng W, Cleland TP, Bern M. 2013 Molecular analyses of dinosaur osteocytes support the presence of endogenous molecules. *Bone* **52**, 414–423. (doi:10.1016/j.bone.2012.10.010)
23. Schweitzer MH, Suo Z, Avci R, Asara JM, Allen MA, Arce FT, Horner JR. 2007 Analyses of soft tissue from *Tyrannosaurus rex* suggest the presence of protein. *Science* **316**, 277–280. (doi:10.1126/science.1138709)
24. Asara JM, Garavelli JS, Slatter DA, Schweitzer MH, Freimark LM, Phillips M, Cantley LC. 2007 Interpreting sequences from mastodon and *T. rex*. *Science* **317**, 1324–1325. (doi:10.1126/science.317.5843.1324)
25. Organ CL, Schweitzer MH, Zheng W, Freimark LM, Cantley LC, Asara JM. 2008 Molecular phylogenetics of mastodon and *Tyrannosaurus rex*. *Science* **320**, 499. (doi:10.1126/science.1154284)
26. Bada JL, Wang XS, Hamilton H. 1999 Preservation of key biomolecules in the fossil record: current knowledge and future challenges. *Phil. Trans. R. Soc. Lond. B* **354**, 77–87. (doi:10.1098/rstb.1999.0361)
27. Lindahl T. 1993 Recovery of antediluvian DNA. *Nature* **365**, 700–700. (doi:10.1038/365700a0)
28. Lindahl T. 1993 Instability and decay of the primary structure of DNA. *Nature* **362**, 709–715. (doi:10.1038/362709a0)
29. Hofreiter M, Serre D, Poinar HN, Kuch M, Paabo S. 2001 Ancient DNA. *Nat. Rev.* **2**, 353–359. (doi:10.1038/35072071)
30. Hoss M. 2000 Neanderthal population genetics. *Nature* **404**, 453–454. (doi:10.1038/35006551)
31. Orlando L *et al*. 2013 Recalibrating *Equus* evolution using the genome sequence of an early Middle Pleistocene horse. *Nature* **499**, 74–78. (doi:10.1038/nature12323)
32. Collins MJ, Gernaey AM, Nielsen-Marsh CM, Vermeer C, Westbroek P. 2000 Slow rates of degradation of osteocalcin: green light for fossil bone protein? *Geology* **28**, 1139–1142. (doi:10.1130/0091-7613(2000)28<1139:srodoo>2.0.co;2)
33. Collins MJ, Riley MS, Child AM, Turner-Walker G. 1995 A basic mathematical simulation of the chemical degradation of ancient collagen. *J. Archaeol. Sci.* **22**, 175–183. (doi:10.1006/jasc.1995.0019)
34. Collins MJ, Waite ER, van Duin ACT. 1999 Predicting protein decomposition: the case of aspartic-acid racemization kinetics. *Phil. Trans. R. Soc. Lond. B* **354**, 51–64. (doi:10.1098/rstb.1999.0359)
35. Allentoft ME *et al*. 2012 The half-life of DNA in bone: measuring decay kinetics in 158 dated fossils. *Proc. R. Soc. B* **279**, 4724–4733. (doi:10.1098/rspb.2012.1745)
36. Eisenstein RS. 2000 Iron regulatory proteins and the molecular control of mammalian iron metabolism. *Annu. Rev. Nutr.* **20**, 627–662. (doi:10.1146/annurev.nutr.20.1.627)
37. Mladěnka P, Šimůnek T, Hübl M, Hrdina R. 2006 The role of reactive oxygen and nitrogen species in cellular iron metabolism. *Free Radic. Res.* **40**, 263–272. (doi:10.1080/10715760500511484)
38. Bellelli A, Brunori M. 2011 Hemoglobin allostery: variations on the theme. *Biochim. Biophys. Acta* **1807**, 1262–1272. (doi:10.1016/j.bbabio.2011.04.004)
39. Michel FM, Hosein HA, Hausner DB, Debnath S, Parise JB, Strongin DR. 2010 Reactivity of ferritin and the structure of ferritin-derived ferrihydrite. *Biochim. Biophys. Acta* **1800**, 871–885. (doi:10.1016/j.bbagen.2010.05.007)
40. Krebs C, Bollinger JMJ, Booker SJ. 2012 Cyanobacterial alkane biosynthesis further expands the catalytic repertoire of the ferritin-like 'di-iron-carboxylate' proteins. *Curr. Opin. Chem. Biol.* **15**, 291–303. (doi:10.1016/j.cbpa.2011.02.019)
41. Theil EC, Behera RK, Tosha T. 2013 Ferritins for chemistry and for life. *Coord. Chem. Rev.* **257**, 579–586. (doi:10.1016/j.ccr.2012.05.013)
42. Theil E. 2007 Coordinating responses to iron and oxygen stress with DNA and mRNA promoters: the ferritin story. *Biometals* **20**, 513–521. (doi:10.1007/s10534-006-9063-6)
43. Shafer FQ, Yui Quian S, Buetter GR. 2000 Iron and free radical oxidations in cell membranes. *Cell. Mol. Biol.* **46**, 657–662.
44. Chua-anusorn W, Webb J. 2000 Infrared spectroscopic studies of nanoscale iron oxide deposits isolated from human thalassemic tissues. *J. Inorg. Biochem.* **79**, 303–309. (doi:10.1016/S0162-0134(99)00233-0)
45. Theil EC, Goss DJ. 2009 Living with iron (and oxygen): questions and answers about iron homeostasis. *Chem. Rev.* **109**, 4568–4579. (doi:10.1021/cr900052g)
46. Liu X, Theil EC. 2005 Ferritins: dynamic management of biological iron and oxygen chemistry. *Acc. Chem. Res.* **38**, 167–175. (doi:10.1021/ar0302336)
47. Mole DR. 2010 Iron homeostasis and its interaction with prolyl hydroxylases. *Antioxid. Redox Signal.* **12**, 445–458. (doi:10.1089/ars.2009.2790)
48. Davis CI, Kausz AT, Zager RA, Kharasch ED, Cochran RP. 1999 Acute renal failure after cardiopulmonary bypass is related to decreased serum ferritin levels. *J. Am. Soc. Nephrol.* **10**, 2396–2402.
49. Theil EC, Matzapetakis M, Liu X. 2006 Ferritins: iron/oxygen biominerals in protein nanocages. *J. Biol. Inorg. Chem.* **11**, 803–810. (doi:10.1007/s00775-006-0125-6)
50. Halliwell B, Gutteridge JM. 1984 Oxygen toxicity, oxygen radicals, transition metals and disease. *Biochem. J.* **219**, 1–14.
51. Loeffler DA, Connor JR, Juneau PL, Snyder BS, Kanaley L, DeMaggio AJ, Nguyen H, Brickman CM, LeWitt PA. 1995 Transferrin and iron in normal, Alzheimer's disease and Parkinson's disease brain regions. *J. Neurochem.* **65**, 710–716. (doi:10.1046/j.1471-4159.1995.65020710.x)
52. Thompson KJ, Shoham S, Connor JR. 2001 Iron and neurodegenerative disorders. *Brain Res. Bull.* **55**, 155–164. (doi:10.1016/S0361-9230(01)00510-X)
53. Eaton JW, Qian M. 2002 Molecular bases of cellular iron toxicity. *Free Radic. Biol. Med.* **32**, 833–840. (doi:10.1016/S0891-5849(02)00772-4)
54. Hawkins CL, Davies MJ. 2001 Generation and propagation of radical reactions on proteins. *Biochim. Biophys. Acta* **1504**, 196–219. (doi:10.1016/S0005-2728(00)00252-8)
55. Dunlop RA, Rodgers KJ, Dean RT. 2002 Recent developments in the intracellular degradation of oxidized proteins. *Free Radic. Biol. Med.* **33**, 894–906. (doi:10.1016/S0891-5849(02)00958-9)
56. Beckman KB, Ames BN. 1998 The free radical theory of aging matures. *Physiol. Rev.* **78**, 547–581.
57. Huang AR, Ponka P. 1983 A study of the mechanism of action of pyridoxal isonicotinoyl hydrazone at the cellular level using reticulocytes loaded with non-heme 59Fe. *Biochim. Biophys. Acta* **757**, 306–315. (doi:10.1016/0304-4165(83)90056-9)
58. Hašková P, Kovaříková P, Koubková L, Vávrová A, Macková E, Šimůnek T. 2011 Iron chelation with salicylaldehyde isonicotinoyl hydrazone protects against catecholamine autoxidation and cardiotoxicity. *Free Radic. Biol. Med.* **50**, 537–549. (doi:10.1016/j.freeradbiomed.2010.12.004)
59. Espósito BP, Epsztejn S, Breuer W, Cabantchik ZI. 2002 A review of fluorescence methods for assessing labile iron in cells and biological fluids. *Anal. Biochem.* **304**, 1–18. (doi:10.1006/abio.2002.5611S0003269702956113[pii])
60. Guilminot E, Dalard F, Degrigny C. 2002 Mechanism of iron corrosion in water-polyethylene glycol (PEG 400) mixtures. *Corros. Sci.* **44**, 2199–2208. (doi:10.1016/s0010-938x(02)00010-0)
61. Toner B, Santelli CM, Marcus MA, Wirth R, Chan CS, McCollum T, Bach W, Edwards KJ. 2009 Biogenic iron oxyhydroxide formation at mid-ocean ridge hydrothermal vents: Juan de Fuca Ridge. *Geochim. Cosmochim. Acta* **73**, 388–403. (doi:10.1016/j.gca.2008.09.035)
62. Rosenbloom J, Abrams WR, Mecham R. 1993 Extracellular matrix 4: the elastic fiber. *FASEB J.* **7**, 1208–1218.
63. Parish CA, Jiang H, Tokiwa Y, Berova N, Nakanishi K, McCabe D, Zuckerman W, Xia MM, Gabay JE. 2001 Broad-spectrum antimicrobial activity of hemoglobin. *Bioorg. Med. Chem.* **9**, 377–382. (doi:10.1016/S0968-0896(00)00263-7)
64. Froidevaux R, Krier F, Nedjar-Arroume N, Vercaigne-Marko D, Kosciarz E, Ruckebusch C, Dhulster P,

Guillochon D. 2001 Antibacterial activity of a pepsin-derived bovine hemolobin fragment. *FEBS Lett.* **491**, 159–163. (doi:10.1016/S0014-5793(01)02171-8)

65. Simoni J, Feola M, Canizaro P. 1990 Generation of free oxygen radicals and the toxicity of hemoglobin solutions. *Biomat. Artif. Cells Artif. Organs* **18**, 189–202.
66. Ryter SW, Tyrrell RM. 2000 The heme synthesis and degradation pathways: role in oxidant sensitivity. *Free Radic. Biol. Med.* **28**, 289–309. (doi:10.1016/S0891-5849(99)00223-3)
67. Bern M, Phinney BS, Goldberg D. 2009 Reanalysis of *Tyrannosaurus rex* mass spectra. *J. Proteome Res.* **8**, 4328–4332. (doi:10.1021/pr900349r)
68. Balla G, Jacob HS, Balla J, Rosenberg M, Nath K, Apple f, Eaton JW, Vercellotti G. 1992 Ferritin: a cytoprotective antioxidant strategem of endothelium. *J. Biol. Chem.* **267**, 18 148–18 153.
69. Balla J, Jacob HS, Balla G, Nath K, Eaton JW, Vercellotti GM. 1993 Endothelial-cell heme uptake from heme proteins: induction of sensitization and desensitization to oxidant damage. *Proc. Natl Acad. Sci. USA* **90**, 9285–9289. (doi:10.1073/pnas.90.20.9285)
70. Aarden EM, Nijweide PJ, Burger EH. 1994 Function of osteocytes in bone. *J. Cell. Biochem.* **55**, 287–299. (doi:10.1002/jcb.240550304)
71. Cowin SC. 2002 Mechanosensation and fluid transport in living bone. *JMNI* **2**, 256–260.
72. Schweitzer MH, Marshall M, Carron K, Bohle DS, Busse SC, Arnold EV, Barnard D, Horner JR, Starkey JR. 1997 Heme compounds in dinosaur trabecular bone. *Proc. Natl Acad. Sci. USA* **94**, 6291–6296. (doi:10.1073/pnas.94.12.6291)
73. Greenwalt DE, Goreva YS, Siljestrom SM, Rose T, Harbach RE. In press. Hemoglobin-derived porphyrins preserved in a Middle Eocene blood-engorged mosquito. *Proc. Natl Acad. Sci. USA* **5**. (doi:10.1073/pnas.1310885110)
74. Lindsey JS, Chandrashaker V, Taniguchi M, Ptaszek M. 2011 Abiotic formation of uroporphyrinogen and coproporphyrinogen from acyclic reactants. *New J. Chem.* **35**, 511–516. (doi:10.1039/c0nj00977f)
75. Gutierrez L, Quintana C, Patino C, Bueno J, Coppin H, Roth MP, Lazaro FJ. 2009 Iron speciation study in Hfe knockout mice tissues: magnetic and ultrastructural characterisation. *Biochim. Biophys. Acta* **1792**, 541–547. (doi:10.1016/j.bbadis.2009.03.007)
76. Dickson DP, Reid NM, Mann S, Wade VJ, Ward RJ, Peters TJ. 1988 Mössbauer spectroscopy, electron microscopy and electron diffraction studies of the iron cores in various human and animal haemosiderins. *Biochim. Biophys. Acta* **957**, 81–90. (doi:10.1016/0167-4838(88)90159-8)
77. Theil EC. 1987 Ferritin: structure, gene regulation, and cellular function in animals, plants, and microorganisms. *Annu. Rev. Biochem.* **56**, 289–315. (doi:10.1146/annurev.bi.56.070187.001445)
78. Dehner C, Morales-Soto N, Behera RK, Shrout J, Theil EC, Maurice PA, Dubois JL. 2013 Ferritin and ferrihydrite nanoparticles as iron sources for *Pseudomonas aeruginosa*. *J. Biol. Inorg. Chem.* **18**, 371–381. (doi:10.1007/s00775-013-0981-9)
79. Turano P, Lalli D, Felli IC, Theil EC, Bertini I. 2010 NMR reveals pathway for ferric mineral precursors to the central cavity of ferritin. *Proc. Natl Acad. Sci. USA* **107**, 545–550. (doi:10.1073/pnas.0908082106)
80. Altman SA, Zastawny TH, Randers-Eichhorn L, Cacciuttolo MA, Akman SA, Dizdaroglu M, Rao G. 1995 Formation of DNA-protein cross-links in cultured mammalian cells upon treatment with iron ions. *Free Radic. Biol. Med.* **19**, 897–902. (doi:10.1016/0891-5849(95)00095-F)
81. Eilert KD, Foran DR. 2009 Polymerase resistance to polymerase chain reaction inhibitors in bone. *J. Forensic Sci.* **54**, 1001–1007. (doi:10.1111/j.1556-4029.2009.01116.x)
82. Alaeddini R. 2012 Forensic implications of PCR inhibition—a review. *Forensic Sci. Int. Genet.* **6**, 297–305. (doi:10.1016/j.fsigen.2011.08.006)
83. Campbell KL *et al*. 2010 Substitutions in woolly mammoth hemoglobin confer biochemical properties adaptive for cold tolerance. *Nat. Genet.* **42**, 536–540. (doi:10.1038/ng.574)
84. Asara JM, Schweitzer MH, Freimark LM, Phillips M, Cantley LC. 2007 Protein sequences from mastodon and *Tyrannosaurus rex* revealed by mass spectrometry. *Science* **316**, 280–285. (doi:10.1126/science.1137614)
85. Schweitzer MH, Horner JH. 1999 Intravascular microstructures in trabecular bone tissues of *Tyrannosaurus rex*. *Ann. Paleontol.* **85**, 179–192. (doi:10.1016/S0753-3969(99)80013-5)
86. Schweitzer MH, Johnson C, Zocco TG, Horner JR, Starkey JR. 1997 Preservation of biomolecules in cancellous bone of *Tyrannosaurus rex*. *J. Vertebr. Paleontol.* **17**, 349–359. (doi:10.1080/02724634.1997.10010979)